

Electron tunneling rate in quantum dots under a uniform electric field

David M.-T. Kuo and Yia-Chung Chang

Department of Physics and Materials Research Laboratory, University of Illinois at Urbana-Champaign, Urbana, Illinois 61801

(Received 1 November 1999; revised manuscript received 6 December 1999)

A stabilization method is used to evaluate the tunneling rate of an electron in isolated quantum dots of conical shape under uniform electric field. A stabilization graph is obtained by plotting the eigenvalues of a single quantum dot embedded in a confining box made of barrier material as functions of the size of the box. The eigenvalues of the system are calculated within the effective mass approximation via the Raleigh-Ritz variational method. The density of states associated with the quasibound state is constructed from the stabilization graph and is shown to have a Lorentzian profile. The width of the Lorentzian profile gives the tunneling rate. We show that the tunneling rate of the quantum dot system is 2–3 times smaller than that of a quantum well system with the same bound-to-continuum transition energy.

I. INTRODUCTION

Recently, self-assembled InAs/GaAs quantum dots grown by molecular beam epitaxy have attracted a great deal of scientific interest.^{1–8} Due to the large lattice mismatch between InAs and GaAs,² the highly strained epitaxial layer of InAs on GaAs has a tendency to form coherent three-dimensional islands after completion of the wetting layer. These InAs islands typically have the shape of pyramids,^{8,9} disks,¹⁰ lenses,^{11,12} or cones.^{13,14} The mechanism of InAs nucleation has been investigated by Tersoff *et al.*¹⁵ and Holy *et al.*¹⁶ Many useful applications of quantum dot (QD) devices have been discussed.^{17,18} One promising application is the quantum dot infrared photodetector (QDIP), in which the bound-to-continuum transition is utilized. The main advantage of the QDIP versus QWIP (quantum well infrared photodetector) is that light can be directly coupled to the electrons in the normal incidence geometry due to the effect of QD confinement in directions perpendicular to the growth axis. For applications as infrared detectors, another important factor to consider is the dark current, which is related to the electron escape rate in the QD under an electric field.

The electron escape rate (inverse of the tunneling time) of quantum well systems has been extensively studied.^{19,20} Theoretical methods for evaluating the electron tunneling rate include the phase-shift method,¹⁹ the complex-energy method,²⁰ and the stabilization method. All these methods give essentially identical results. In the phase-shift approach, the eigenfunction of the Hamiltonian for the QW system under an electric field is solved analytically and the lifetime of the quasibound state is related to the inverse of the width of the local density of states (LDOS) as a function of energy. At low fields, this resonance profile is well approximated by a Lorentzian function. Thus, it is expected that a complex-energy solution to the time-independent Schrödinger equation with proper boundary condition²⁰ will give rise to the same lifetime as the quasibound state. Both the phase-shift method and the complex-energy method require solving the wave functions of the system. On the other hand, the stabilization method requires finding only the eigenvalues of the system Hamiltonian as functions of an external parameter (the scaling factor), which allows evaluation of the LDOS

via integration over the external parameter and subtracting the background contribution.

Extensive theoretical studies of the electronic and optical properties of QDs have been performed by several groups.^{21–25} However, no theoretical studies of the electron tunneling rate for quantum dots of realistic geometry have been reported to date. In light of the promising IR detector application of QD systems, it is desirable to investigate the electron tunneling rate, so that the dark current of the QD device can be assessed. There are three different mechanisms that contribute to the dark current of QDs: thermionic, phonon-assisted tunneling, and direct tunneling. Based on calculations on quantum well systems,²⁶ we expect the direct tunneling process to dominate at medium to high fields. In this paper, we report a theoretical study of the electron tunneling rate of an InAs/GaAs conical QD, since it determines the direct tunneling current. Here the stabilization method (SM) is used rather than the phase-shift or complex-energy method, since accurate numerical solution to the eigenstates of the QD system under an electric field as a continuous function of energy is difficult to obtain because of the low symmetry of the system.

The stabilization graph (SG) was introduced by Simons for finding the resonance energy and width of a metastable state.²⁷ A SG is generated by plotting the energy eigenvalues of the system subject to the variation of a scaling factor, which is taken to be the size of a confining box with infinite potential. The eigenvalues of the system can be solved numerically via the Raleigh-Ritz variational method. Using the SG, one can determine the energy width of the metastable state by relating it to the energy separation between eigenvalues for states near the resonance based on Fermi's golden rule (FGR).^{28,29} Such a method has been applied frequently to various quantum systems.^{30,31} Using the FGR method for the SG, Borondo and Dehesa³² calculated the energy and widths of resonances of an isolated quantum well in an electric field. Although the FGR method gives a reasonable estimate of the resonance width, the result obtained depends on the size of the confining box used.³² Thus, the method is not very accurate, especially at high fields where the higher-order contributions become important.

On the other hand, Mandelshtam *et al.*³³ constructed an

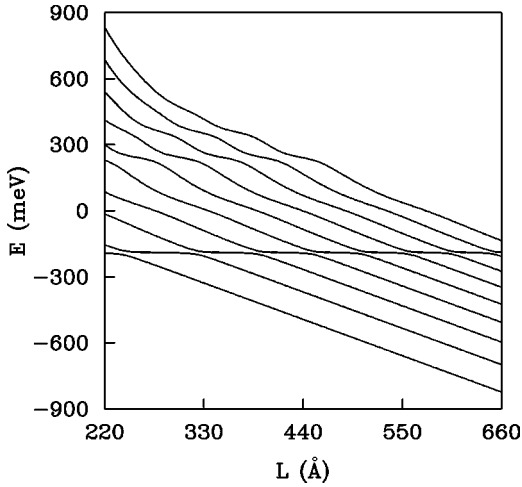


FIG. 1. Energy eigenvalues of an $\text{Al}_{0.3}\text{Ga}_{0.7}\text{As}/\text{GaAs}$ quantum well with well width 51 \AA under an electric field ($F=300 \text{ kV/cm}$) as functions of the scale factor L .

accurate numerical method which allows the extraction of the local density of states for the metastable states of the system from the SG. The LDOS obtained has a well-defined Lorentzian profile and its width is insensitive to the size of the confining box used. In this paper, we shall apply this method to both quantum well and quantum dot systems. We show that applying this method to quantum well system gives results for the resonance width in excellent agreement with those obtained via the phase-shift method. Thus, we believe that this method is capable of obtaining accurate results for the electron tunneling time for quantum dot systems as well.

II. QUANTUM WELL SYSTEM

To test the accuracy of the stabilization method used, we shall first apply the method to a one-dimensional QW system. This allows a detailed comparison of results obtained by both the SM and the phase-shift method. A brief discussion of the SM is given in the appendix. We consider a single $\text{Al}_{0.3}\text{Ga}_{0.7}\text{As}/\text{GaAs}/\text{AlGaAs}$ quantum well system with well width $d=51 \text{ \AA}$. The effective masses for GaAs and $\text{Al}_{0.3}\text{Ga}_{0.7}\text{As}$ used in our calculation are $m_w^*=0.067m_e$ and $m_B^*=0.095m_e$ (m_e is the bare electron mass), respectively. The conduction band offset used is $V_0=-247 \text{ meV}$. The above set of parameters gives two bound states in the well with energies $E_0=-174 \text{ meV}$ and $E_1=-4 \text{ meV}$ in the absence of field. These values are obtained by solving the transcendental equation for the quantum well, taking into account the difference of effective masses for GaAs and AlGaAs. To solve the problem in the presence of an electric field, we place the quantum well at the center of a confining box with width L and infinite potential barrier. The uniform electric field of strength F introduces an additional term $-eF(z-L/2)$ to the Hamiltonian, where e is the electron charge and z is the coordinate along the growth axis. A basis set of up to 70 sine functions $\phi_m(x)=\sqrt{2/L}\sin(k_m z)$ ($k_m=m\pi/L, m=\text{positive integers}$) is used to construct the eigenfunctions of the system. Here the origin ($z=0$) is defined to be at the left corner of the confining box. The matrix

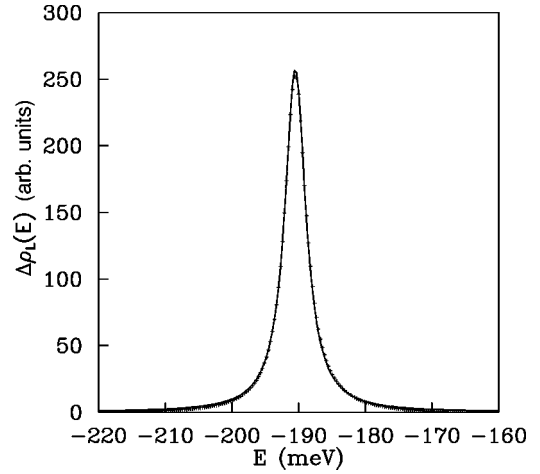


FIG. 2. Background-subtracted SDOS [$\Delta\rho_L(E)$] for an $\text{Al}_{0.3}\text{Ga}_{0.7}\text{As}/\text{GaAs}$ quantum well with width 51 \AA under an electric field ($F=300 \text{ kV/cm}$). The curve is fitted with a Lorentzian function (solid line) with $E_r=-190.5 \text{ meV}$ and width $\Gamma=3.82 \text{ meV}$.

elements of the Hamiltonian can be calculated analytically. The lowest two eigenvalues of H in the absence of field obtained by numerical diagonalization are found to agree with the analytical results (which were obtained by solving a transcendental equation) within 0.1 meV , indicating the convergence of the basis set used.

Figure 1 shows the stabilization graph for $F=300 \text{ kV/cm}$, in which the lowest ten eigenvalues of H are plotted as functions of the scaling factor L . A resonance state at energy near -200 meV is quite apparent as the horizontal line intertwined with many slanting lines (due to continuum states outside the well). The minigaps at the anticrossing points indicate the coupling strength between the quasibound state and the continuum states.

Using the SM, we obtain the size-averaged density of states (SDOS) as defined in the Appendix. The result is shown in Fig. 2. 440 mesh points for L ranging from 220 to 660 \AA were used to perform the average. The curve is well fitted by a Lorentzian function (solid curve) with resonance energy $E_r=-190.5 \text{ meV}$ and width $\Gamma=3.82 \text{ meV}$. The result agrees well with that obtained by the phase-shift method (see Table I). However, at lower fields, this procedure does not work so well without substantially increasing the number of basis functions. At lower fields, the first crossover between the quasibound state and continuum states occurs at a

TABLE I. Resonance energy (E_r) and width (Γ) of an $\text{Al}_{0.3}\text{Ga}_{0.7}\text{As}/\text{GaAs}$ quantum well with well width 51 \AA at various fields.

Electric field F (kV/cm)	Phase shift		Stabilization method			
	E_r (meV)	Γ (meV)	$N=70$		$N=140$	
			E_r (meV)	Γ (meV)	E_r (meV)	Γ (meV)
150	-178	0.0354	-178	0.028	-178	0.032
200	-181	0.397	-181	0.374	-181	0.388
250	-185	1.60	-185	1.584	-185	1.592
300	-190	3.98	-191	3.888	-191	3.942
350	-195	7.59	-196	7.378	-196	7.4

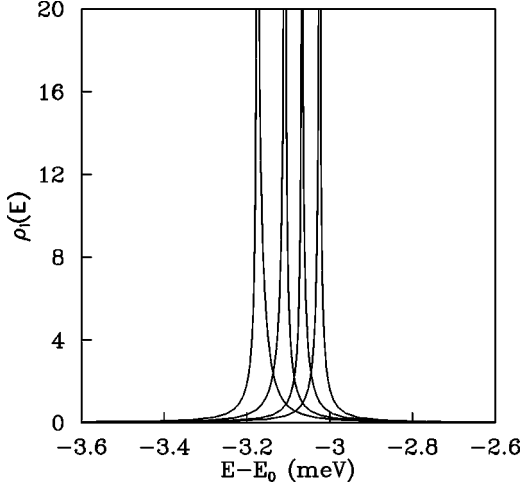


FIG. 3. Contributions to the background-subtracted SDOS for an $\text{Al}_{0.3}\text{Ga}_{0.7}\text{As}/\text{GaAs}$ quantum well (with well width 51 \AA) under an electric field ($F=150 \text{ kV/cm}$) due to various branches, where $E_0 = -175 \text{ meV}$.

much larger value of L . Thus, a much larger basis set is needed. This is undesirable, since it will make application of this method to the quantum dot system difficult. If we keep the number of basis functions fixed at 70, the resulting resonance energy E_r will shift upward as L increases, and the SDOS will be artificially broadened when we average over L . This is better illustrated by rewriting the SDOS as

$$\rho_L(E) = \frac{1}{\Delta L} \sum_i \rho_i(E),$$

where

$$\rho_i(E) = \left. \frac{dE_i(L)}{dL} \right|_{E_i(L_0)=E}^{-1} \quad \text{with } L < L_0 < L + \Delta L.$$

In Fig. 3, we plot $\rho_i(E)$ versus E for $i=2, \dots, 5$ for $F=150 \text{ kV/cm}$. We see in this figure that $\rho_i(E)$ are all well described by Lorentzian profiles, but their center $E_r^{(i)}$ has shifted upward as i increases from 2 to 5. The shift in $E_r^{(i)}$ is larger than the width of the Lorentzian profile, which leads to a substantial error in the estimated resonance width when one sums over i . The problem gets worse as the field is further reduced. To circumvent this problem, we define a corrected SDOS as

$$\bar{\rho}_L(E) = \frac{1}{\Delta L} \sum_i \rho_i(E - E_r^{(i)}), \quad (1)$$

where the Lorentzian profiles for all branches are rigidly shifted, so they are all centered at the same energy. The width of $\bar{\rho}_L(E)$ will be closer to the actual resonant width than that of the uncorrected LDOS $[\rho_L(E)]$.

In low fields there is another problem that can also cause numerical error in the estimate of Γ . The slope $dL/dE_i(L)$ is nearly divergent at $E = E_r^{(i)}$ when the resonance width is extremely small, which can lead to large numerical errors in evaluating $\rho_i(E)$ at E near E_r . This problem has been overcome by Ravuri, Mandelshtam, and Taylor,³⁴ they reconstructed the phase shift from the SDOS by integration over

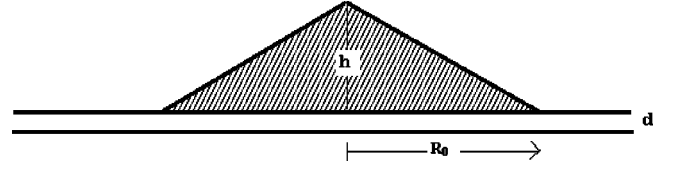


FIG. 4. Schematic diagram for a conical InAs/GaAs quantum dot with height 35 \AA , base radius 52.5 \AA , and wetting layer 5 \AA .

E . Here we introduce a simpler method to overcome this problem at low fields. The idea is based on the observation that the resonance energy $E_r^{(i)}$ of each curve for $\rho_i(E)$ can be determined rather precisely, although the value of $\rho_i(E)$ itself at $E_r^{(i)}$ is subject to large numerical error. Therefore, we define the energy-weighted SDOS as

$$\eta_L(E) = \frac{1}{\Delta L} \sum_i (E - E_r^{(i)}) [\rho_i(E - E_r^{(i)}) - \rho^0]. \quad (2)$$

Here ρ^0 is the background contribution, which is essentially a constant. Since $[\rho_i(E - E_r^{(i)}) - \rho^0]$ should be a Lorentzian function, $\eta_L(E)$ can be well fitted by the function $CE/[E^2 + (\Gamma/2)^2]$. The function has a minimum at $-\Gamma/2$ and a maximum at $\Gamma/2$. The energy separation between the minimum and maximum of $\eta_L(E)$ gives the value of Γ directly, and no fitting is necessary. We found the method introduced here works quite well in determining the resonance width with the use of a fixed number (taken to be 70) of basis functions even at low fields ($F \approx 200 \text{ kV/cm}$). A comparison of results at various fields obtained by the present method (with either 70 or 140 basis functions) and the phase-shift method is given in Table I. The agreement between the two methods is within 6% (2%) for fields $\geq 200 \text{ kV/cm}$ when 70 (140) basis functions are used. Note that at the smallest field $F=150 \text{ kV/cm}$, 140 basis functions are still not enough to provide accurate value for τ . The error in this case is near 10% in comparison with the phase-shift method.

III. QUANTUM DOT SYSTEM

A schematic diagram of the conical QD considered here is shown in Fig. 4. The Hamiltonian of an isolated conical QD with wetting layer can be expressed by^{13,14} (in cylindrical coordinates)

$$H_0 = \frac{-\hbar^2}{2} \left(\frac{\partial}{\partial z} \frac{1}{m^*(z,r)} \frac{\partial}{\partial z} \right) + \frac{-\hbar^2}{2} \left(\frac{1}{r} \frac{\partial}{\partial r} \frac{r}{m^*(z,r)} \frac{\partial}{\partial r} \right) + \frac{1}{m^*(z,r)} \frac{1}{r^2} \frac{\partial^2}{\partial \phi^2} + V(z) + \Delta V(z,r), \quad (3)$$

where the spatially dependent effective mass is given by

$$m^*(z,r)^{-1} = m_G^*{}^{-1} [\theta(-z) + \theta(z-D) + \theta(D-z)\theta(z-d)\theta(r-r_c(z))] + m_I^*{}^{-1} [\theta(z)\theta(d-z) + \theta(D-z)\theta(z-d)\theta(r_c(z)-r)], \quad (4)$$

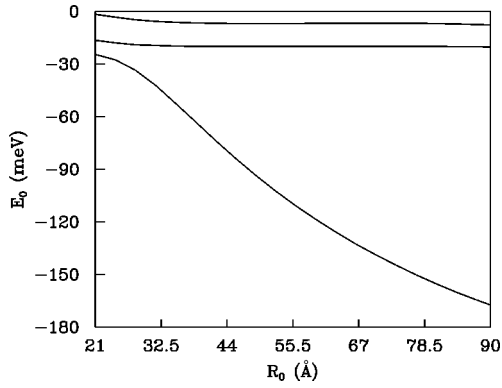


FIG. 5. Energies of the bound states of a conical quantum dot as functions of the base radius.

$$V(z) = \begin{cases} -V_0 & \text{for } 0 \leq z \leq d \\ 0 & \text{otherwise,} \end{cases} \quad (5)$$

and

$$\Delta V(z, r) = -V_0 \theta(z-d) \theta(D-z) \theta(r_c-r), \quad (6)$$

with

$$r_c(z) = (D-z) \tan(\theta_0).$$

$m_G^* = 0.067m_e$ and $m_I^* = 0.024m_e$ are the effective masses of GaAs and InAs, respectively, $\theta(x)$ is a step function, V_0 is the conduction-band offset, and $D = d + h$, where d and h are the thickness of the wetting layer and the height of the conical QD, respectively. $\tan(\theta_0) = R_0/h$, where R_0 is the radius of the conical QD base. Note that the spin-orbit interaction has been ignored in the Hamiltonian of Eq. (3). Similarly to the quantum well system, we introduce a set of square integrable basis functions, which are eigenfunctions of a cylindrical box of radius R ($R \gg R_0$) and length L ($L \gg d$) with infinite potential barrier:

$$\phi_{n,m}(r, z) = \beta_n J_0(k_n r) \sin[k_m(z + L/2)], \quad (7)$$

where

$$\beta_n = \frac{\sqrt{2}}{\sqrt{\pi L}} \frac{1}{R J_1(k_n R)}$$

is the normalization factor. $k_m = m\pi/L$, and $k_n R$ is the n th zero of the Bessel function $J_0(x)$. Only cylindrically symmetric basis functions are considered here, because we are interested only in the states that can be coupled to the quibound state when the electric field is applied in the z direction (which still preserves the cylindrical symmetry). The same set of basis functions has been used by Marzin and Bastard¹³ to calculate the quantum confined states in a conical QD. The expression of the matrix elements of the Hamiltonian of Eq. (3) can be readily obtained. Seventy sine functions multiplied by ten Bessel functions are used to diagonalize the Hamiltonian. The convergence is checked by increasing the basis functions and with the current set of bases the ground state energy is accurate to within 1 meV.

Figure 5 shows the energy levels of the confined states as a function of the base radius (R_0) of the conical dot. The other material parameters used here are the wetting layer

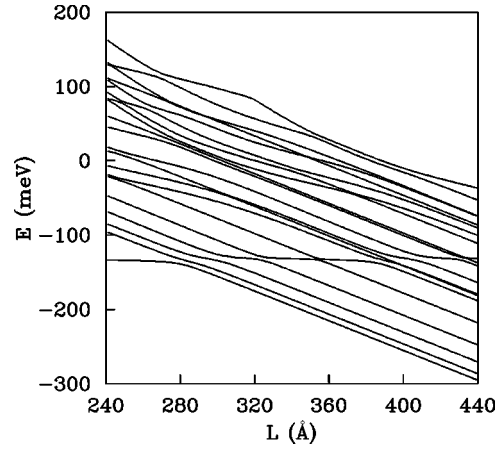


FIG. 6. Energy eigenvalues of a conical InAs/GaAs quantum dot under an electric field ($F = 200$ kV/cm) as functions of the scale factor L .

thickness $d = 5$ Å, the height of the cone $h = 35$ Å, the conduction-band offset $V_0 = 0.5$ eV (this includes the effect of hydrostatic strain due to the lattice mismatch between InAs and GaAs), the radius of the confining cylinder $R = 400$ Å, and the length of the confining box $L = 400$ Å. Three bound states are found for the range $R_0 = 20$ – 90 Å. For detector application, we are seeking an intersubband transition at an energy around 0.1 eV, which occurs at $R_0 = 52.5$ Å, where the three bound states are at energies -1.024 , -0.020 , and -0.007 eV.

In the presence of the electric field, a potential term $-eFz$ is added to the Hamiltonian H_0 , which leads to a Stark shift and finite lifetime for the confined states. To evaluate the energy and width of resonant states of the quantum dot, we shall use the corrected SDOS method discussed above.

Figure 6 shows the stabilization graph for a conical QD under field $F = 200$ kV/cm. All material parameters used are the same as in Fig. 5 with $R_0 = 52.5$ Å and the length of the confining box L varying from 240 to 440 Å. The current set of parameters gives a bound-to-continuum transition energy around 102 meV, which is designed for application for 10 μm infrared radiation detection. Using Eq. (2), we obtain the energy-weighted SDOS, $\eta_L(E)$ as shown in Fig. 7. The resonance width obtained by taking the energy separation between minimum and maximum of $\eta_L(E)$ is 2.28 meV. We have calculated the Stark shift and resonance width of the conical QD at various fields. The results are listed in Table II. For comparison, we also include the results for an $\text{Al}_{0.3}\text{Ga}_{0.7}\text{As}/\text{GaAs}$ quantum well with well width $d = 24$ Å. This well width is chosen so that the bound-to-continuum transition energies are also around 102 meV.

Figure 8 shows the comparison of the electron tunneling rate ($1/\tau = \Gamma/\hbar$) as a function of field (F) for a conical InAs/GaAs QD and an $\text{Al}_{0.3}\text{Ga}_{0.7}\text{As}/\text{GaAs}$ QW. We see in the figure that the electron tunneling rate of the QD is consistently lower than that in the QW, although their bound-to-continuum transition energies are almost the same. Since the tunneling rate determines the dark current due to the direct tunneling process, our study indicates that a QDIP has some advantage over a QWIP because of its lower dark current.

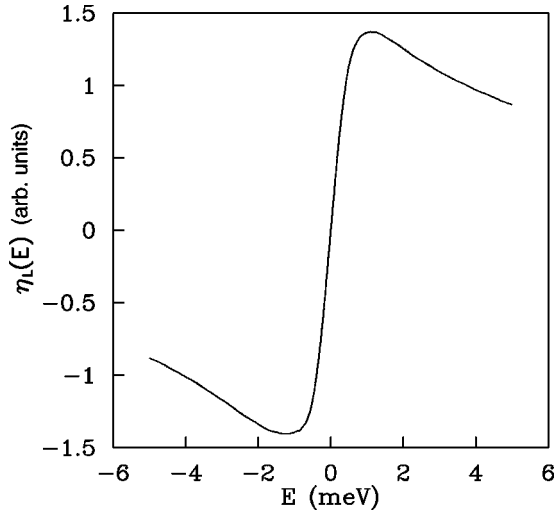


FIG. 7. Energy-weighted SDOS $\eta_L(E)$ [defined in Eq. (2)] for a conical InAs/GaAs quantum dot under an electric field ($F=200$ kV/cm).

IV. SUMMARY

In this article we studied the energy and width of the quasibound states of isolated quantum well and quantum dot systems under an electric field via a stabilization method. From the stabilization graph (eigenvalues plotted as functions of a scaling factor L), we constructed the size-average density of states, which is well fitted by Lorentzian functions with width corresponding to the tunneling rate. Our study shows that the electron escape rate (which determines the dark current) of quantum dots with conical shape is smaller than that of quantum wells with the same bound-to-continuum transition energy by a factor 2–3. This suggests that the dark current for quantum-dot-based infrared detectors will be significantly lower than that for the quantum-well based infra-red detectors when the direct tunneling mechanism is dominant. Although we studied only quantum dots of conical shape, the same conclusion is expected to be applicable to quantum dots of other shapes (pyramidal, lenslike, or disklike).

Throughout this paper, we have considered only the low-concentration limit, in which no two electrons will occupy the quantum dot at the same time. Thus, the correlated effect due to the electron-electron interaction can be ignored. This electron-electron interaction can lead to a Coulomb blockade which will affect the transport properties of quantum dots^{35–38} in the case that each quantum dot contains a few electrons. The effect of Coulomb blockade on the electron

TABLE II. Resonance energy (E_r) and width (Γ) of an InAs/GaAs conical quantum dot and an $\text{Al}_{0.3}\text{Ga}_{0.7}\text{As}$ /GaAs quantum well with well width 24 Å at various fields.

Electric field F (kV/cm)	Quantum dot		Quantum well	
	E_r (meV)	Γ (meV)	E_r (meV)	Γ (meV)
125	-120.2	0.278	-118.3	0.799
150	-125.1	0.660	-122.4	1.920
200	-135.3	2.28	-131.1	5.376
250	-147.2	5.16	-140.0	10.10

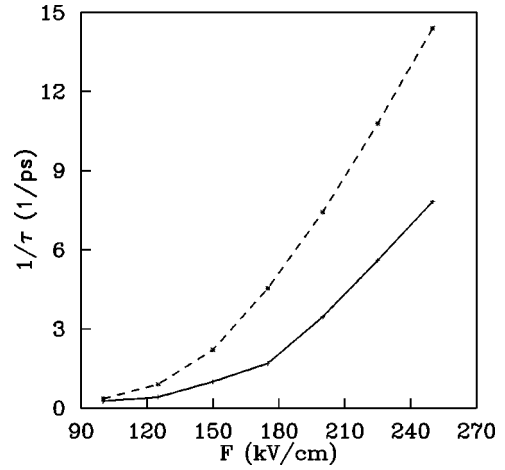


FIG. 8. Electron tunneling rate $1/\tau$ versus electric field F for an InAs/GaAs conical quantum dot (solid line) and an $\text{Al}_{0.3}\text{Ga}_{0.7}\text{As}$ /GaAs quantum well with well width 24 Å (dashed line). Both systems have a bound-to-continuum transition energy around 102 meV.

escape rate in quantum dots will be a subject of our future studies.

ACKNOWLEDGMENTS

This work was supported by a subcontract from the University of Southern California under the MURI program, AFOSR, Contract No. F49620-98-1-0474.

APPENDIX: THE STABILIZATION METHOD

In this appendix, we briefly discuss the stabilization method used by Mandelshtam *et al.*³³ One way to calculate the lifetime of a metastable state of a system is to find the localized density of states confined in the region (Ω) of interest:

$$\rho_{\Omega}(E) = \sum_i \int_{\mathbf{r} \in \Omega} |\psi_i(\mathbf{r})|^2 d^3\mathbf{r} \delta(E - E_i). \quad (\text{A1})$$

For a metastable state with sufficiently long lifetime, $\rho_{\Omega}(E)$ is well described by a Lorentzian shape centered at a resonance energy (E_r) with width Γ . For a system with infinite size, an infinite number of basis functions is required to obtain the exact result. Numerically, one can truncate the system at a finite size and use a finite number of basis functions. Or, equivalently, one places the system in a confining box of length L in each direction. The number of basis functions required to yield the desired numerical accuracy should increase with the size L . Plotting the energy eigenvalues versus the size L typically produces a stable horizontal line (corresponding to the metastable state) intertwined with many closely spaced curves (corresponding to continuum states). Such a graph is called the stabilization graph, and allows immediate identification of the resonance energy and a rough estimate of the resonance width by evaluating the energy spacing between the resonance level and nearby continuum states. However, to obtain an accurate evaluation of the resonance width, one needs a numerically smooth resonance profile for $\rho_{\Omega}(E)$, which requires knowing $\rho_{\Omega}(E)$ on a fine

energy grid with spacing much smaller than the resonance width Γ . Since Γ can be very small for a metastable system with a long lifetime, the size L required to produce a fine energy spacing is often very large, which leads to too large a value of N to allow practical calculation.

Mandelstam, Ravuri, and Taylor³³ have developed a simple method for extracting the LDOS from the stabilization graph. They define a size-averaged density of states (SDOS) as

$$\begin{aligned} \rho_L(E) &\equiv \frac{1}{\Delta L} \int_L^{L+\Delta L} dL \sum_i \delta(E - E_i(L)) \\ &= \frac{1}{\Delta L} \sum_i \left| \frac{dE_i(L)}{dL} \right|^{-1}_{E_i(L_0)=E} \\ &\quad \times \theta(L < L_0 < L + \Delta L), \end{aligned} \quad (\text{A2})$$

where $\theta(L < L_0 < L + \Delta L) = 1$ if $L < L_0 < L + \Delta L$ and zero otherwise. Unlike the LDOS defined in Eq. (A1), this quantity is a numerically smooth function of E , since one can choose a fine mesh in L when performing the integral over L in Eq. (A2). $\rho_L(E)$ has a maximum at the resonance energy E_r where $|dE_i(L)/dL|$ is a minimum. Subtracting the background contribution (due to continuum states) to the SDOS, one obtains a potential-well-induced change in the SDOS,

$$\Delta \rho_L(E) = \rho_L(E) - \rho_L^0(E),$$

where $\rho_L^0(E)$ is the background contribution, which can be obtained by removing the potential well in the Hamiltonian. It can be shown that $\Delta \rho_L(E)$ is rather insensitive to the size L ,³³ as long as L is a few times larger than the length of Ω , although $\rho_L(E)$ keeps increasing with L . So one can obtain a stable $\Delta \rho_L(E)$ for a moderate size of L .

-
- ¹L. Goldstein, F. Glas, J. Y. Marzin, M. N. Charasse, and G. Leroux, *Appl. Phys. Lett.* **47**, 1099 (1985).
²D. J. Eaglesham and M. Cerullo, *Phys. Rev. Lett.* **64**, 1943 (1990).
³C. W. Snyder, B. G. Orr, D. Kessker, and L. M. Sander, *Phys. Rev. Lett.* **66**, 3032 (1991).
⁴J. Y. Marzin, J. M. Gerard, A. Izrael, D. Barrier, and G. Bastard, *Phys. Rev. Lett.* **73**, 716 (1994).
⁵Q. Xie, A. Madhukar, P. Chen, and N. P. Kobayashi, *Phys. Rev. Lett.* **75**, 2542 (1995).
⁶G. S. Solomon, J. A. Trezza, and J. S. Harris, *Appl. Phys. Lett.* **66**, 991 (1995).
⁷G. S. Solomon, J. A. Trezza, A. F. Marshall, and J. S. Harris, Jr., *Phys. Rev. Lett.* **76**, 952 (1996).
⁸M. Grundman, J. Christen, N. N. Ledentsov, J. Bohrer, D. Bimberg, S. S. Ruvimov, P. Werner, U. Richter, U. Gosele, J. Heydenreich, V. M. Ustinov, A. Y. Egorov, A. E. Zhukov, P. S. Kopev, and Z. I. Alferov, *Phys. Rev. Lett.* **74**, 4043 (1995).
⁹M. Grundmann, O. Stier, and D. Bimberg, *Phys. Rev. B* **52**, 11 969 (1995).
¹⁰F. M. Peeters and A. Schweigert, *Phys. Rev. B* **53**, 1460 (1996).
¹¹S. Fafard, R. Leon, D. Leonard, J. L. Merz, and P. M. Petroff, *Phys. Rev. B* **52**, 5752 (1995).
¹²H. Drexel, D. Leonard, W. Hansen, J. P. Kotthaus, and P. M. Petroff, *Phys. Rev. Lett.* **73**, 2252 (1994).
¹³J. Y. Marzin and G. Bastard, *Solid State Commun.* **92**, 437 (1994).
¹⁴P. Lelong and G. Bastard, *Solid State Commun.* **98**, 819 (1995).
¹⁵J. Tersoff, C. Teichert, and M. G. Lagally, *Phys. Rev. Lett.* **76**, 1675 (1996).
¹⁶V. Holy, G. Springholz, M. Pinczolit, and G. Bauer, *Phys. Rev. Lett.* **83**, 356 (1999).
¹⁷Y. Arakawa and H. Sakaki, *Appl. Phys. Lett.* **40**, 939 (1982).
¹⁸Q. Xie, A. Kalburge, P. Chen, and A. Madhukar, *IEEE Photonics Technol. Lett.* **8**, 965 (1996).
¹⁹E. J. Austin and M. Jaros, *Phys. Rev. B* **31**, 5569 (1985).
²⁰D. Ahn and S. L. Chung, *Phys. Rev. B* **34**, 9034 (1986).
²¹M. A. Cusack, P. R. Briddon, and M. Jaros, *Phys. Rev. B* **54**, 2300 (1996).
²²K. Chang and J. B. Xia, *Solid State Commun.* **104**, 351 (1997).
²³S. S. Li and J. B. Xia, *Phys. Rev. B* **55**, 15 434 (1997).
²⁴L. W. Wang, J. Kim, and A. Zunger, *Phys. Rev. B* **59**, 5678 (1999).
²⁵A. Franceschetti, H. Fu, L. W. Wang, and A. Zunger, *Phys. Rev. B* **60**, 1819 (1999).
²⁶D. M. T. Kuo and Y. C. Chang, *Phys. Rev. B* **60**, 15 957 (1999).
²⁷J. Simons, *Chem. Phys. Lett.* **75**, 2465 (1981).
²⁸W. H. Miller, *Chem. Phys. Lett.* **4**, 627 (1970).
²⁹M. F. Fels and A. U. Hazi, *Phys. Rev. A* **4**, 662 (1970).
³⁰A. U. Hazi and M. F. Fels, *Chem. Phys. Lett.* **8**, 582 (1971).
³¹M. F. Fels and A. U. Hazi, *Phys. Rev. A* **5**, 1236 (1972).
³²F. Borondo and J. S. Dehesa, *Phys. Rev. B* **33**, 8758 (1986).
³³V. A. Mandelshtam, T. R. Ravuri, and H. S. Taylor, *Phys. Rev. Lett.* **70**, 1932 (1993).
³⁴T. R. Ravuri, V. A. Mandelshtam, and H. S. Taylor, *Superlattices Microstruct.* **20**, 87 (1996).
³⁵D. Goldhaber-Gordon, H. Schtrikman, D. Mahalu, D. Abusch-Magder, U. Meirau, and M. A. Kastner, *Nature (London)* **391**, 156 (1998).
³⁶S. M. Cronenwett, T. H. Oosterkamp, and L. P. Kouwenhoven, *Science* **281**, 540 (1998).
³⁷A. Kaminski, I. L. Aleiner, and L. I. Glazman, *Phys. Rev. Lett.* **81**, 685 (1998).
³⁸Y. Meir, N. S. Wingreen, and P. A. Lee, *Phys. Rev. Lett.* **66**, 3048 (1991).